

Novel Key Metabolites Reveal Further Branching of the Roquefortine/Meleagrins Biosynthetic Pathway*

Received for publication, October 7, 2013, and in revised form, November 11, 2013. Published, JBC Papers in Press, November 13, 2013, DOI 10.1074/jbc.M113.512665

Marco I. Ries^{†1,2}, Hazrat Ali^{§¶1,3}, Peter P. Lankhorst^{||}, Thomas Hankemeier^{†***}, Roel A. L. Bovenberg^{||††}, Arnold J. M. Driessen^{§¶}, and Rob J. Vreeken^{†***4}

From the [†]Division of Analytical Biosciences, Leiden Academic Centre for Drug Research, Einsteinweg 55, 2333CC Leiden, the [§]Department of Molecular Microbiology, Groningen Biomolecular Sciences and Biotechnology Institute, Zernike Institute for Advanced Materials, University of Groningen, Nijenborgh 7, 9747AG Groningen, the [¶]Kluyver Centre for Genomics of Industrial Fermentations, Julianalaan 67, 2628BC Delft, the ^{||}DSM Biotechnology Center, Alexander Fleminglaan 1, 2613AX Delft, the ^{**}Netherlands Metabolomics Centre, Leiden University, Einsteinweg 55, 2333CC Leiden, and the ^{††}Department of Synthetic Biology and Cell Engineering, Groningen Biomolecular Sciences and Biotechnology Institute, University of Groningen, Nijenborgh 7, 9747AG Groningen, The Netherlands

Background: The fungal roquefortine/meleagrins gene cluster is a source of diverse bioactive molecules.

Results: Novel metabolites of the roquefortine/meleagrins biosynthetic pathway were discovered, and synthetase genes were assigned to biosynthetic reactions.

Conclusion: Distinctive unspecificity of modifying enzymes leads to excessive branching in the pathway, resulting in various intermediates and products.

Significance: Metabolites from the roquefortine/meleagrins gene cluster have potential antimicrobial and chemotherapeutic application.

Metabolic profiling and structural elucidation of novel secondary metabolites obtained from derived deletion strains of the filamentous fungus *Penicillium chrysogenum* were used to reassign various previously ascribed synthetase genes of the roquefortine/meleagrins pathway to their corresponding products. Next to the structural characterization of roquefortine F and neoxaline, which are for the first time reported for *P. chrysogenum*, we identified the novel metabolite roquefortine L, including its degradation products, harboring remarkable chemical structures. Their biosynthesis is discussed, questioning the exclusive role of glandicoline A as key intermediate in the pathway. The results reveal that further enzymes of this pathway are rather unspecific and catalyze more than one reaction, leading to excessive branching in the pathway with meleagrins and neoxaline as end products of two branches.

The filamentous fungus *Penicillium chrysogenum* has been commercially exploited for many decades due to its high production of β -lactam antibiotics such as penicillin G (1). Next to penicillins, secondary metabolites such as roquefortines and glandicolines were isolated from liquid cultures of *P. chrysogenum*, which show pharmaceutically interesting properties, such as neurotoxic (2), antimicrobial (3, 4), and antitumor (5) activ-

ities. They are structurally closely related and arise from the roquefortine/meleagrins pathway, which contains a dimodular nonribosomal peptide synthetase flanked by six associated genes (6, 7). Starting with histidyltryptophanyldiketopiperazine (HTD),⁵ synthesized by the core synthetase enzyme RoqA using tryptophan and histidine as substrates, RoqD catalyzes the reversed prenylation of HTD at the C-3 of its indole moiety, utilizing dimethylallyl diphosphate to form roquefortine D. At the same time, RoqR, a cytochrome P450 oxidoreductase, oxidizes HTD at its histidinyl moiety to dehydrohistidyltryptophanyldiketopiperazine (DHTD). Both simultaneous reactions of HTD lead to a branch of the roquefortine/meleagrins pathway, one to DHTD via the oxidation by RoqR and further to roquefortine C by dimethylallyl addition of RoqD, and the other via an alteration of the enzymatic order. There, dimethylallyl addition is first performed by RoqD to yield roquefortine D, whereas further oxidation is carried out by RoqR, yielding roquefortine C (see Fig. 1). Although several labeling, silencing, and deletion experiments have been conducted, there is still ambiguity about the subsequent biosynthetic reactions and the genes involved. For instance, roquefortine C is supposed to be converted into glandicoline A and further to glandicoline B with RoqM and RoqO each catalyzing one reaction (6, 7). However, their assignment to a particular reaction is still unclear. In addition, neoxaline was proposed as final product of the pathway, originating from a hydrogenation of meleagrins (8), yet no gene could be found in the *roq* gene cluster performing that reaction.

Here, we describe the quantification, structural identification, and biosynthesis of five previously unidentified metabolites, obtained from highly sensitive comparative metabolite

* This work was supported by the Perspective Genbiotics program subsidized by Stichting toegepaste wetenschappen (STW) and (co)financed by the Netherlands Metabolomics Centre (NMC), which is a part of the Netherlands Genomics Initiative/Netherlands Organization for Scientific Research.

¹ Both authors contributed equally to this work.

² Supported by the STW.

³ Present address: Center for Biotechnology and Microbiology, University of Swat, 19130 Odigram, Pakistan. Supported by the Higher Education Committee of Pakistan (HEC) and STW.

⁴ To whom correspondence should be addressed. E-mail: vreekenrj@lacdr.leidenuniv.nl.

⁵ The abbreviations used are: HTD, histidyltryptophanyldiketopiperazine; DHTD, dehydrohistidyltryptophanyldiketopiperazine; HMBC, heteronuclear multiple bond correlation; calc., calculated.

Novel Key Metabolites in the Roquefortine/Meleagrins Pathway

profiling of host and deletion strains. Roquefortine F and neoxaline, next to the three structurally novel compounds, which we named roquefortine L, M, and N, were found to be derived from the roquefortine/meleagrins pathway. These results demonstrate a further branching of this secondary metabolite pathway yielding a variety of intermediates with complex structures and a diverse range of activities.

EXPERIMENTAL PROCEDURES

Host Strains, Media, Grown Conditions, and Plasmid Construction—*P. chrysogenum* strain DS54555, which lacks both the penicillin cluster genes and the *ku70* gene, was used as a host strain for deletion analysis and was kindly supplied by DSM Anti-infective (Delft, The Netherlands). All the strains were grown on YGG medium for protoplast formation and transformation. For analysis, cells were grown on secondary metabolite production medium (7) (glucose, 5.0 g/liter; lactose, 75 g/liter; urea, 4.0 g/liter; Na₂SO₄, 4.0 g/liter; CH₃COONH₄, 5.0 g/liter; K₂HPO₄, 2.12 g/liter; KH₂PO₄, 5.1 g/liter) for secondary metabolite production using a shaking incubator at 200 rpm for 168 h at 25 °C.

Metabolite Profiling—All strains used for gene assignments were grown in quintuplicate to increase statistical power, according to the procedure described above. Sample preparation was carried out as described previously (7). Metabolomic profiling was performed on an Agilent 1200 capillary pump (Agilent, Santa Clara, CA) coupled to a Surveyor photodiode array detector (Thermo Scientific) and an LTQ-FT-ICR-Ultra mass spectrometer (Thermo Scientific) equipped with an electrospray interface as described earlier (7).

Metabolite Identification—The identity of compound **10** was confirmed by comparing retention time and MS fragmentation spectra to its commercially available standard, purchased from Bio-Connect (Huissen, The Netherlands). Compounds **6**, **9**, **11**, and **12** were identified using NMR after extraction from liquid cultures. **6** was extracted from the *roqN* deletion strain culture filtrate, which was made alkaline with 25% ammonium hydroxide (pH 10) and extracted with dichloromethane. The alkaline dichloromethane layer was evaporated to dryness, redissolved in water containing 50% acetonitrile, vortexed, centrifuged, and transferred to an autosampler vial for fraction collection via preparative reversed phase LC on an Atlantis T3 column (10 × 100 mm, 5 μm) (Waters, Milford, MA). Compound **9** was extracted following the isolation procedure above except using culture filtrate of the *roqO* deletion strain, whereas **11** and **12** were obtained from the same culture filtrate after lyophilization and extraction using methanol. The methanol layer was evaporated to dryness, redissolved in water, vortexed, centrifuged, and subjected to repeated semipreparative chromatography as described above. Elemental composition of compounds **6**, **9**, **11**, and **12** was determined using high-resolution MS. NMR spectra were recorded on a Bruker Avance III 700 MHz or 600 MHz spectrometer with sample temperatures ranging from 260 to 300 K, depending on the particular requirements for each sample. By choosing an optimal acquisition temperature, severe line broadening could be avoided, which was observed for various signals due to conformational averaging. For acquisition, samples were dissolved in equal amounts of dimethyl sulfoxide (DMSO) and CDCl₃.

Chemical Stability of Compound 6—An aqueous solution of compound **6** was adjusted to pH 2.5 by the addition of formic acid. Metabolite profiling was carried out as described above. Products, formed by a degradation of **6**, were compared with extracted standards using HPLC-MS/MS.

RESULTS

Metabolite Profiling of Host and Deletion Strains Leads to Five New Metabolites of the Roquefortine/Meleagrins Pathway—In a previous study, we described the identification of various abundant metabolites and resolved the major enzymatic steps belonging to the roquefortine/meleagrins pathway (7). To identify secondary metabolites originating from the *roq* gene cluster (Fig. 1A), culture supernatants of the host strain and individually *roq* gene deletion strains were subjected to comparative metabolite profiling using HPLC-UV-MS (Fig. 2). As host strain, *P. chrysogenum* DS54555, which is derived from the industrial DS17690 strain lacking the *ku70* gene and multiple penicillin biosynthetic genes clusters, was used. Here, we describe the identification and quantification of several less abundant metabolites, roquefortine L (**6**), roquefortine F (**9**), neoxaline (**10**), roquefortine M (**11**), and roquefortine N (**12**) (Fig. 1B), that have not been previously considered or structurally characterized, filling missing biosynthetic reaction steps in the roquefortine/meleagrins pathway.

Structure Elucidation and Quantification of 6, 11, and 12—Compound **6** is a novel complex metabolite composed of a roquefortine scaffold and a rare nitron moiety, thus named roquefortine L. The mass-to-charge ratio of its corresponding ion was observed at 404.1706 using HPLC-FT-ICR-MS, representing the protonated molecule [M+H]⁺ with formula C₂₂H₂₂N₅O₃ (calc. 404.1717) eluting at 16.8 min. The same ion was previously tentatively identified as glandicoline A (**13**) (Fig. 1B) as elemental composition and parts of the structure indicated consistency with this compound (7). However, its ¹H and ¹³C NMR data showed high similarity to the diketopiperazine **4**, indicating a roquefortine-like core structure. Furthermore, its ¹H NMR spectrum revealed two protons at C-8 representing a single bond between C-8 and C-9, which is different from the double bond described for **13** (Table 1). Additionally, C-2 (δ_C = 146) in the ¹³C HMBC spectrum indicated a double bond between N-1 and C-2, which was supported by the chemical shift of N-1 (δ_N = 280) in the ¹⁵N HMBC spectrum. As compound **13** was reported from various *Penicillium* species such as *Penicillium albocoremium* (8), *Penicillium glandicola* (9), and *P. chrysogenum* (10) and proposed as a precursor of **7**, host and *roq* deletion strain chromatograms of *P. chrysogenum* were further analyzed for the presence of **13**. The chromatogram of the ion with *m/z* 404.1706, representing the protonated molecule [M+H]⁺ with formula C₂₂H₂₂N₅O₃ of both compound **6** and compound **13**, was extracted in a 5-ppm mass accuracy window. However, no ion possibly corresponding to **13** could be found, whereas **6** was observed at high concentration in the liquid media (Fig. 3). The absence of **13** in host and various *P. chrysogenum* strains lead to the conclusions that **13** is not produced by *P. chrysogenum* DS54555.

Compounds **11** and **12** are novel compounds based on a roquefortine-like scaffold, thus named roquefortine M and

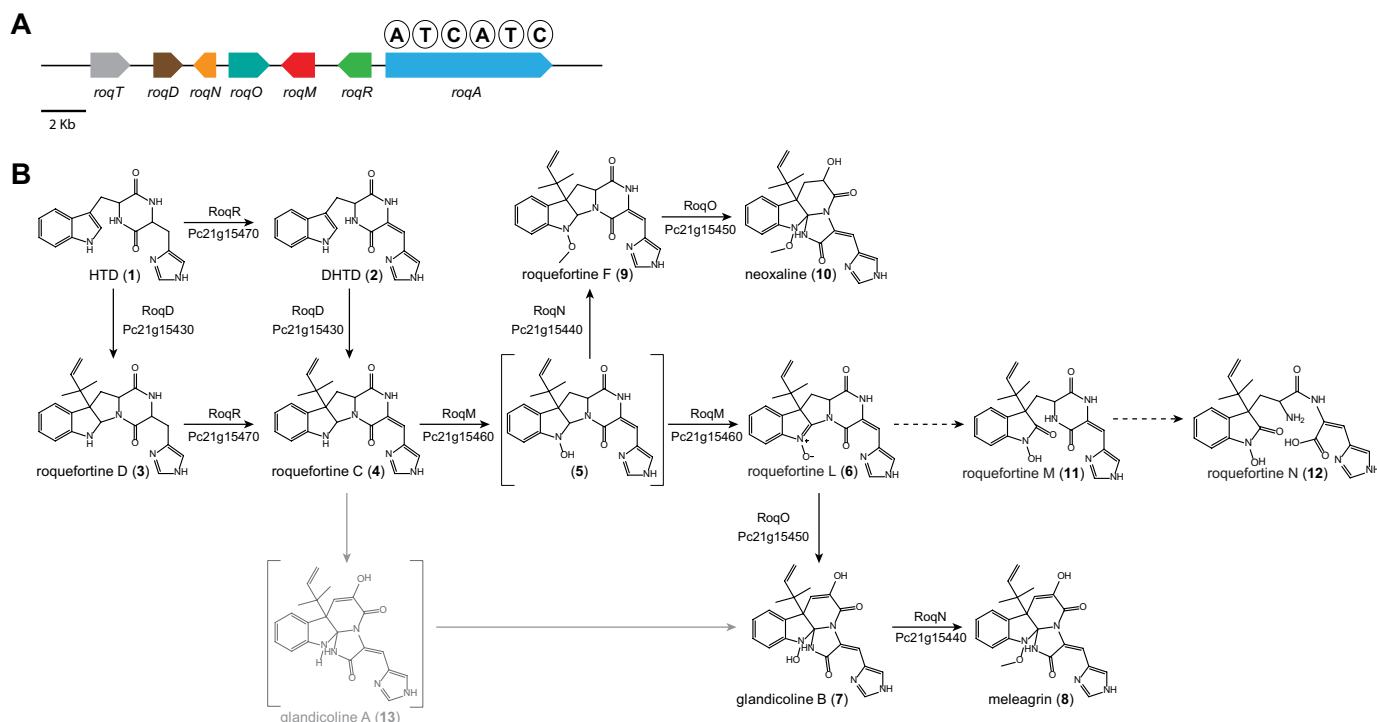


FIGURE 1. Roquefortine/meleagrins biosynthetic gene cluster and proposed corresponding pathway. *A*, organization of the roquefortine/meleagrins biosynthetic gene cluster. *B*, proposed roquefortine/meleagrins pathway. Numbers between brackets are compound identifiers used throughout this study. Enzymatic catalyzed reactions are indicated by solid arrows, whereas chemical reactions are indicated by dashed arrows. Structures shown in brackets could not be detected, whereas gray reactions and compounds were previously proposed for various *Penicillium* species (6, 8, 10).

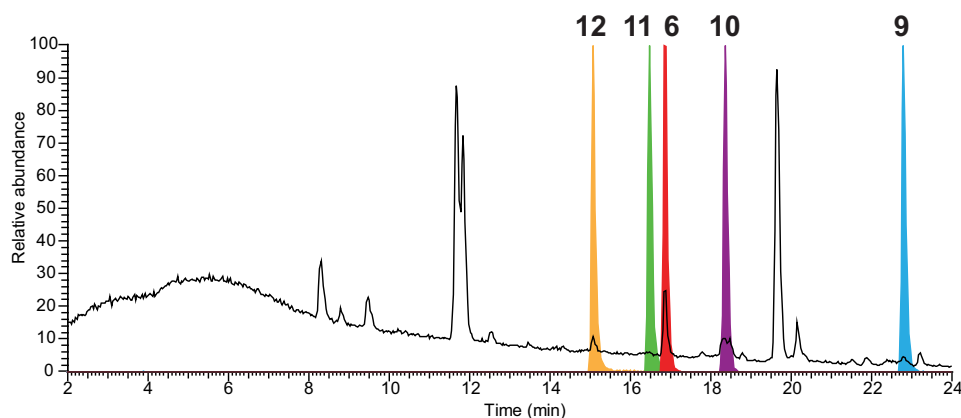


FIGURE 2. HPLC-MS elution profiles of novel metabolites of the meleagrins/neoxaline pathway. The HPLC-MS total ion chromatogram (black) and normalized extracted ion chromatograms (colored) of the novel secondary metabolites roquefortine N (**12**, 15.1 min), roquefortine M (**11**, 16.5 min), roquefortine L (**6**, 16.8 min), neoxaline (**10**, 17.8 min), and roquefortine F (**9**, 22.8 min) from the meleagrins/neoxaline pathway are shown.

roquefortine N. High-resolution electrospray ionization mass spectrometry of **11** (m/z 422.1814 $[M+H]^+$, calc. 422.1824) and **12** (m/z 440.1918 $[M+H]^+$, calc. 440.1928) established the molecular formula $C_{22}H_{23}N_5O_4$ and $C_{22}H_{25}N_5O_5$. Their chemical structure was determined using ^{13}C HMBC, ^{15}N HMBC, and 1H NMR (Table 2) showing similar signals as observed for compound **6**, which indicates a similar chemical scaffold. However, the significant upfield shift of N-1 (from $\delta_N = 280$ in **6** to $\delta_N = 185$ in **11**) in the ^{15}N HMBC spectra together with the chemical shift of C-2 ($\delta_C = 146$ in **6**, $\delta_C = 172$ in **11**) in the ^{13}C NMR spectra of compound **11** shows that **11** contains a single bond between N-1 and C-2, with C-2 being a carbonylic carbon. In addition, a comparison between the ^{15}N HMBC spectrum of compounds **11** and **12** revealed that the amide bond between

N-14 and C-13 in **11** was hydrolyzed in **12** ($\delta_N = 32.0$), yielding a primary amine and a carboxyl group. Both compounds commonly occur, together with compound **6**, in liquid cultures of *P. chrysogenum* host and *roqT*, *roqN*, and *roqO* deletion strains (Fig. 3). Their absence in the remaining deletion strain samples concludes the involvement of *roqA*, *roqR*, *roqD*, and *roqM* in their biosynthesis.

Structure Elucidation and Quantification of 9 and 10—Compound **9** with molecular formula $C_{23}H_{25}N_5O_3$, established by high-resolution electrospray ionization mass spectrometry (m/z 420.2015 $[M+H]^+$, calc. 420.2030), was identified as roquefortine F, a metabolite solely reported from a deep ocean sediment-derived *Penicillium* species (11), using 1H and ^{13}C NMR (Table 1). Its 1H NMR spectrum is very similar to the

Novel Key Metabolites in the Roquefortine/Meleagrins Pathway

spectrum of **3** (7), except for a double bond between C-12 and C-15. Furthermore, the presence of C-26 ($\delta_C = 63.6$) in the ^{13}C NMR spectrum, next to a sharp OCH_3 peak ($\delta_H = 4.01$) and a missing proton on N-1 in the ^1H NMR spectrum, fully agrees with a methoxylated N-1 in compound **9**. This was supported by the absence of correlations with a carbon or proton in the HMBC spectrum. The concentration of **9**, particularly high in the host strain, was found to be reduced to approximately one-

third in the deletion strains of *roqT* and *roqO* and absent in the remaining deletion strains (Fig. 3). These data suggest that *roqO* and *roqT* are the only two genes not involved in the biosynthesis of **9**. Compound **10** with molecular formula $\text{C}_{23}\text{H}_{25}\text{N}_5\text{O}_4$ (m/z 436.1967 $[\text{M}+\text{H}]^+$, calc. 436.1979) was identified as neoxaline, a metabolite previously isolated from *Aspergillus japonicus* Fg-551 (12) and *Penicillium tulipae* (13), by comparing retention time and MS/MS fragments with its commercially available standard. Although the concentration of **10** in host and *roqT* deletion strain is almost comparable, a 97% decrease was

TABLE 1

Chemical shifts of ^1H , ^{13}C , and ^{15}N NMR of roquefortine L (**6**) and ^1H and ^{13}C NMR of roquefortine F (**9**) (δ in ppm)

roquefortine L (6)			roquefortine F (9)		
	290 K	280 K	290 K	280K	280K
	δ_H	δ_C	δ_N	δ_H	δ_C
1-NO	-		280		
2		147.6		5.78	84.9
3		58.2		3	60.5
3a		137.9		3a	130.5
4	7.49	124.3		4	124.5
5	7.44	129.0		5	124.4
6	7.52	128.6		6	128.8
7	7.56	114.9		7	116.0
7a		148.5		7a	150.9
8	2.24, 2.95	24.5		8	37.7
9	5.06	63.6		9	57.4
10		164.9		10	164.5
11-NH	10.77		136	11-NH	10.63
12		122.2		12	*
13		156.7		13	157.4
14-N			127	14-N14	
15	6.57	112.2		15	6.44
16		124.3		16	*
17-N			*	18	7.75
18	7.76	136.3		19-NH	12.82
19-NH	12.42**		*	20	7.21
20	7.49	132.1		21	40.5
21		43.1		22	5.99
22	5.79	141.5		23	5.09, 5.16
23	5.06, 5.09	116.2		24	0.94
24	0.86	22.4		25	1.07
25	1.09	22.3		26	4.01

(*) Not observed.

(**) From spectrum at 280 K.

TABLE 2

Chemical shifts of ^1H , ^{13}C , and ^{15}N NMR of roquefortine M (**11**) and roquefortine N (**12**) (δ in ppm)

roquefortine M (11)			roquefortine N (12)			
	270K	300K	270K	280K	280K	300K
	δ_H	δ_C	δ_N	δ_H	δ_C	δ_N
1-NOH	10.56		185***	10.64**		*
2		172.6			173.1	
3		65.9			54.5	
3a		124.7			124.7	
4	7.20	125.1		7.18	125.0	
5	7.02	121.6		6.99	121.1	
6	7.27	128.2		7.22	127.6	
7	6.95	106.8		6.93	106.4	
7a		142.9			142.7	
8	2.32, 2.60	35.6		2.09, 2.58	35.0	
9	3.20	52.3		2.74	52.6	
10		165.1			*	
11-NH	10.44		137	10.08**		*
12		121.0			*	
13		160.1			*	
14-NH	7.38		118	14-NH ₂	6.57**	30
15	6.26	108.7		8.02	107.1	
16		125.3			127.7	
17-N			262			*
18	7.65	136.4		8.00	133.4	
19-NH	12.87		169	*		196
20	7.09	133.8		7.18	127.6	
21		41.9			41.7	
22	6.00	142.3		6.03	142.5	
23	4.98, 5.09	113.9		4.98, 5.09	113.4	
24	1.04	21.7		1.07	21.4	
25	0.96	21.3		0.98	21.2	

(*) Not observed.

(**) Tentative assignment.

(***) From spectrum at 290 K.

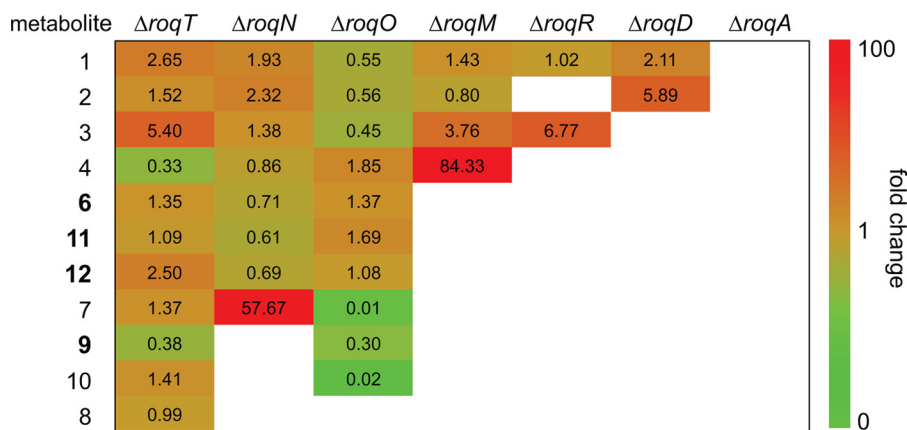


FIGURE 3. -Fold change of the concentration of secondary metabolites from the roquefortine/meleagrins pathway in deletion strains as compared with the host strain. Numbers in the table represent the internal standard corrected concentrations of secondary metabolites in supernatants of deletion strains obtained from HPLC-UV-MS as compared with their concentration in the supernatant of the host strain *P. chrysogenum* DS54555. Cell coloring, representing the -fold change, was performed on a logarithmic scale. Red cells indicate a concentration increase, whereas green cells represent a decrease. White cells indicate a complete absence of the metabolite in the deletion sample. Novel metabolites of the roquefortine/meleagrins pathway are shown with bold numbers.

observed in the *roqO* deletion strain (Fig. 3). In all remaining deletion strains, compound **10** could not be detected, leading to the conclusion that all genes in the *roq* gene cluster, except *roqT*, are required for the synthesis of **10**.

Chemical Degradation of Compound 6 Leads to Various Products—Nitrones, such as compound **6**, are not infinitely stable and degrade already at room temperature in aqueous solution as well as under acidic conditions by incorporation of water (14–16). To determine the resulting degradation products, an aqueous solution of **6** was acidified, and the resulting sample was measured using HPLC-UV-MS (Fig. 4). Next to a 50% decrease of **6**, two highly abundant ions were observed in the treated sample corresponding to **11** and **12**. Additionally, a third unidentified compound was found eluting at 17.33 min with a mass-to-charge ratio of 422.1823, representing the protonated molecule with the formula $C_{22}H_{24}N_5O_4$. These results demonstrate that **11**, **12**, and an unidentified third compound are produced by degradation of the rather unstable compound **6**.

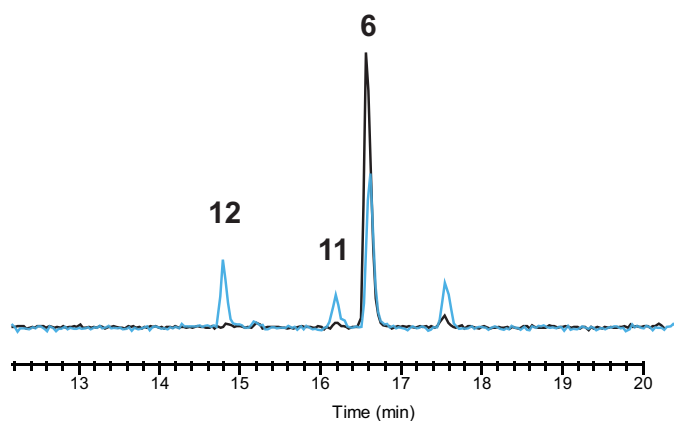


FIGURE 4. Chemical degradation of compound 6 leads to various products. The total ion chromatograms of pure (black) and degraded (blue) compound **6**, after the addition of formic acid, measured on HPLC-MS are shown. Acid-induced degradation leads to the formation of **11** and **12** next to an unidentified compound eluting at 17.33 min with $[M+H]^+ = 422.1823$ and elemental composition $C_{22}H_{23}N_5O_4$.

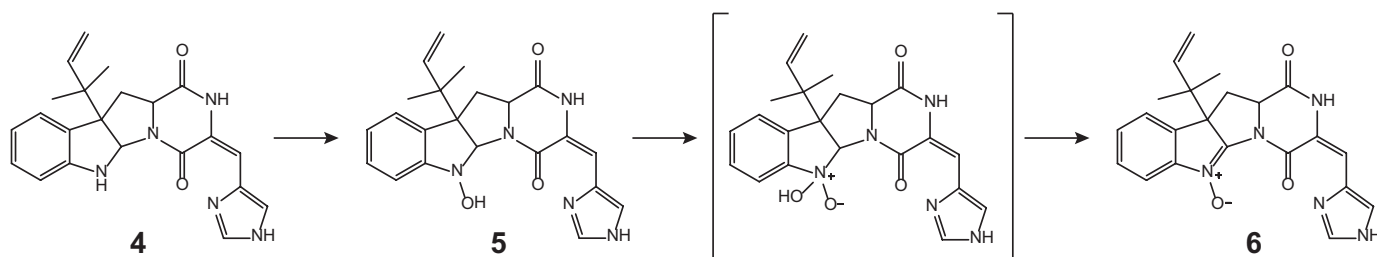


FIGURE 5. Proposed biosynthesis of compound 6 by RoqM.

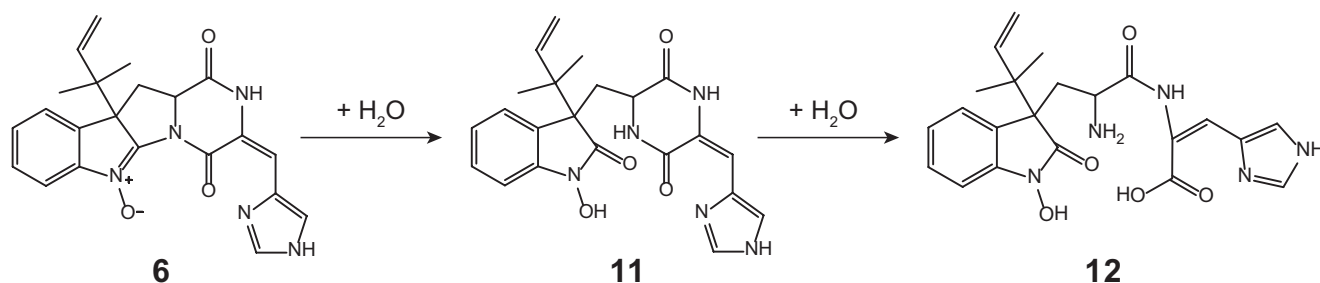


FIGURE 6. Degradation of compound 6 yielding 11 and 12 by consecutive incorporation of water.

DISCUSSION

Here, we present new insight into the complex biosynthesis of secondary metabolites from the roquefortine/meleagrins pathway. Five novel metabolites were found to originate from the *roq* gene cluster, obtained from comparative metabolites profiling of the host strain and various deletion strains in combination with NMR- and MS-based structure elucidation. As all five metabolites are produced in a late stage of the pathway, no changes were observed for the biosynthesis of upstream metabolites **1–4**, which starts with RoqA taking L-histidine and L-tryptophan as substrates and producing compound **1**. Based on the highly significant accumulation of **4** in the *roqM* deletion strain and the absence of all downstream metabolites **6–12** (Fig. 3), it can be concluded that *roqM*, encoding a flavin-dependent MAK 1-monooxygenase-like protein, is involved in the conversion of **4** into **6**, a novel compound containing an unusual nitronium moiety. Nitrones are widely known due to their free radical-trapping properties and their potential application as therapeutics in age-related diseases (17) such as cancer (18) and ischemic stroke (19). As the chemical scaffold of compound **6** is closely related to the roquefortine group, it was named roquefortine L. Flavin-containing monooxygenases are commonly known to consecutively oxidize drugs and xenobiotics containing a soft nucleophile, such as nitrogen or sulfur (20). In the case of secondary amines, flavin-containing monooxygenases consecutively oxidize the nitrogen, leading to the production of hydroxylamines and nitrones (14–16). A similar mechanism for the synthesis of the nitronium-containing compound **6** is very likely, starting with the oxidation of the secondary amine in the indole part of **4**, yielding the hydroxylated intermediate **5** (Fig. 5). Further oxidation on the same nitrogen produces an unstable *N,N*-dihydroxylated species, which is followed by the loss of water, eventually producing compound **6**. However, nitrones are not indefinitely stable and easily degrade at room temperature in aqueous solutions (14–16). Under acidic conditions, compound **6** decomposes by a consecutive incorpora-

tion of water leading, among others, to the production of compounds **11** and **12** (Fig. 4 and 6). This decomposition was also observed in NMR experiments after extended storage of a solution of **6** at room temperature. These results suggest that the presence of **11** and **12** in liquid cultures of *P. chrysogenum* can be attributed to a chemical degradation of **6**. Compound **6**, with the formula $C_{22}H_{21}N_5O_3$, is represented by an ion with a mass-to-charge ratio of 404.1706 and eluting at 16.8 min. The exact same ion was previously tentatively identified as compound **13** (7) as its elemental composition, and parts of the structure indicated consistency with this compound. However, further structure elucidation using various NMR experiments confirmed the structure of **6** instead. This was surprising as compound **13**, a proposed key intermediate in the biosynthesis of downstream metabolites such as **7**, **8**, and **10**, was previously tentatively identified in different *Penicillium* cultures (8, 10). By using a comparable instrumental setup with a similar chromatographic separation method, host and deletion strains of DS54555 were screened for production of **13**. Nevertheless, neither **13** nor corresponding degradation products could be detected, whereas **6** was found at high concentrations, leading to the conclusion that **13** is not produced by *P. chrysogenum*. This is remarkable as **13** was expected as single precursor of **7**, modified by RoqO (6). In addition, a deletion of *roqO* resulted in an up to 98% decrease of **7**, whereas the levels of upstream metabolites remained nearly unchanged, indicating that RoqO is indeed involved in the synthesis of **7**. Due to the general absence of **13** in the *P. chrysogenum*-derived samples, compound **7** has to originate from a different biosynthetic route than the previously reported oxidation of **13** on its indole nitrogen (6–8). RoqO, encoding a P450 monooxygenase, closely resembles FtmG (64% identity, 79% similarity at the amino acid level), a cytochrome P450 monooxygenase catalyzing the hydroxylation of fumitremorgin C to dihydroxy-fumitremorgin C (21), compounds that are structurally similar to the roquefortine derivatives. A possible deduced biosynthesis of **7** involves the hydroxylation of **6** on C-9 by RoqO, comparable with the oxidation of fumitremorgin C by FtmG. Subsequent cleavage of the bond between C-9 and N-14 followed by the development of a bond between C-2 and N-11 is postulated to ultimately yield **7**, similar to the mechanism previously proposed for **13** from **4** (22). These results, together with the general absence of **13** in *P. chrysogenum*, lead to the conclusion that **7** and **8** are produced via a different biosynthesis in *P. chrysogenum* than in other *Penicillium* strains such as *P. tulipae* (8), for which a tentatively identified **13** was reported as intermediate.

The deletion of *roqN* resulted in an accumulation of **7** in the liquid medium, whereas metabolites **8**, **9**, and **10** were absent (Fig. 3). RoqN, a methyltransferase, was previously recognized to catalyze the addition of a methyl group on the hydroxylated nitrogen of **7**, producing **8** (6, 7). As **9** contains a methylated hydroxylamine group in the same position as **8**, the hydroxylamine containing compound **5**, which differs only in a methyl group, is proposed as its direct precursor with RoqN catalyzing the methyl addition to yield **9**. These results reveal a further branching of the roquefortine/meleagrins pathway with compounds **6** and **9** being products of **5**. In addition, they support

the presence of **5**, which was proposed based on its involvement in the biosynthesis of **6**.

Compound **10** was previously proposed as direct product of **8** by enzymatic hydrogenation (8). However, BLAST analysis did not reveal an enzyme in the roquefortine/meleagrins pathway that is able to perform that reaction (6, 7). Moreover, a 53 times higher concentration of **8** as compared with **10** in the host strain, but the absence of **8** in the *roqO* deletion strain with **10** still being present, leads to the conclusion that **8** is not a precursor of **10** (Fig. 3). In contrast, due to the high concentration of **9** in the $\Delta roqO$ strain and its roquefortine-like structure (roquefortine scaffold with a methoxy group on N-1), compound **9** is proposed as direct precursor of **10** with RoqO catalyzing this reaction, similar to the synthesis of **7** from **6**. These results suggest that RoqO is involved in the reactions from **6** into **7** and from **9** into **10** by oxidizing and subsequently converting a roquefortine scaffold into a glandicoline-like structure (Fig. 1B).

In conclusion, these results extend the additional branch of compound **9** leading to the final product **10**. Unspecificity, already observed for RoqR and RoqD (7), could now also be observed for RoqO and RoqN, leading to a complex degree of branching in the pathway and a wide palette of compounds. Several of the new compounds identified in the current study were found to be equipped with interesting biological activities. Roquefortine F, previously reported from a deep ocean sediment-derived fungus *Penicillium* sp., shows moderate cytotoxicity against various tumor cell lines (11). Neoxaline, which was first isolated from *A. japonicas* Fg-551, stimulates the central nervous system in mice (12) and inhibits cell proliferation (23). Furthermore, it was found to induce cell cycle arrest at the G₂/M phase in Jurkat cells (inhibition of tubulin polymerization) (23). Here, the novel metabolites roquefortine L, roquefortine M, and roquefortine N are added to the palette of potential cytotoxic compounds, which demonstrates the potential of engineered industrial *P. chrysogenum* strains to produce novel bioactive compounds with unusual chemical scaffolds.

Acknowledgments—We thank Drs. H. Menke, W. Heijne, and H. Roubos from the DSM Biotechnology Centre for making the DNA microarray data available.

REFERENCES

- Weber, S. S., Polli, F., Boer, R., Bovenberg, R. A., and Driessen, A. J. (2012) Increased penicillin production in *Penicillium chrysogenum* production strains via balanced overexpression of isopenicillin N acyltransferase. *Appl. Environ. Microbiol.* **78**, 7107–7113
- Scott, P. M., Merrien, M. A., and Polonsky, J. (1976) Roquefortine and isofumigaclavine A, metabolites from *Penicillium roqueforti*. *Experientia* **32**, 140–142
- Koolen, H. H., Soares, E. R., Silva, F. M., Souza, A. Q., Medeiros, L. S., Filho, E. R., Almeida, R. A., Ribeiro, I. A., Pessoa Cdo, Ó., Morais, M. O., Costa, P. M., and Souza, A. D. (2012) An antimicrobial diketopiperazine alkaloid and co-metabolites from an endophytic strain of *Gliocladium* isolated from *Strychnos cf. toxifera*. *Nat. Prod. Res.* **26**, 2013–2019
- Clark, B., Capon, R. J., Lacey, E., Tennant, S., and Gill, J. H. (2005) Roquefortine E, a diketopiperazine from an Australian isolate of *Gymnoascus reessii*. *J. Nat. Prod.* **68**, 1661–1664
- Du, L., Feng, T., Zhao, B., Li, D., Cai, S., Zhu, T., Wang, F., Xiao, X., and Gu, Q. (2010) Alkaloids from a deep ocean sediment-derived fungus *Penicil-*

- lium* sp., and their antitumor activities. *J. Antibiot.* **63**, 165–170
6. García-Estrada, C., Ullán, R. V., Albillos, S. M., Fernández-Bodega, M. Á., Durek, P., von Döhren, H., and Martín, J. F. (2011) A single cluster of coregulated genes encodes the biosynthesis of the mycotoxins roquefortine C and meleagrins in *Penicillium chrysogenum*. *Chem. Biol.* **18**, 1499–1512
 7. Ali, H., Ries, M. I., Nijland, J. G., Lankhorst, P. P., Hankemeier, T., Bovenberg, R. A., Vreeken, R. J., and Driessen, A. J. (2013) A branched biosynthetic pathway is involved in production of roquefortine and related compounds in *Penicillium chrysogenum*. *PLoS One* **8**, e65328
 8. Overy, D. P., Nielsen, K. F., and Smedsgaard, J. (2005) Roquefortine/oxaline biosynthesis pathway metabolites in *Penicillium* ser. *Corymbifera*: in planta production and implications for competitive fitness. *J. Chem. Ecol.* **31**, 2373–2390
 9. Kozlovskii, A. G., Vinokurova, N. G., Reshetilova, T. A., Sakharovskii, V. G., Baskunov, B. P., and Seleznev, S. G. (1994) New metabolites of *Penicillium glandicola* var. *glandicola* - glandicoline A and glandicoline B. *Appl. Biochem. Microbiol.* **30**, 334–337
 10. Vinokurova, N. G., Boichenko, L. V., and Arinbasarov, M. U. (2003) Production of alkaloids by fungi of the genus *Penicillium* grown on wheat grain. *Appl. Biochem. Microbiol.* **39**, 403–406
 11. Du, L., Li, D., Zhu, T., Cai, S., Wang, F., Xiao, X., and Gu, Q. (2009) New alkaloids and diterpenes from a deep ocean sediment derived fungus *Penicillium* sp. *Tetrahedron* **65**, 1033–1039
 12. Hirano, A., Iwai, Y., Masuma, R., Tei, K., and Omura, S. (1979) Neoxaline, a new alkaloid produced by *Aspergillus japonicus*. Production, isolation and properties. *J. Antibiot.* **32**, 781–785
 13. Overy, D. P., Phipps, R. K., Frydenvang, K., and Larsen, T. O. (2006) epi-Neoxaline, a chemotaxonomic marker for *Penicillium tulipae*. *Biochem. Syst. Ecol.* **34**, 345–348
 14. Cashman, J. R., Xiong, Y. N., Xu, L., and Janowsky, A. (1999) *N*-Oxygenation of amphetamine and methamphetamine by the human flavin-containing monooxygenase (form 3): role in bioactivation and detoxication. *J. Pharmacol. Exp. Ther.* **288**, 1251–1260
 15. Sun, H., Ehlhardt, W. J., Kulanthaivel, P., Lanza, D. L., Reilly, C. A., and Yost, G. S. (2007) Dehydrogenation of indoline by cytochrome P450 enzymes: a novel “aromatase” process. *J. Pharmacol. Exp. Ther.* **322**, 843–851
 16. Rodriguez, R. J., Proteau, P. J., Marquez, B. L., Hetherington, C. L., Buckholz, C. J., and O’Connell, K. L. (1999) Flavin-containing monooxygenase-mediated metabolism of *N*-deacetyl ketoconazole by rat hepatic microsomes. *Drug Metab. Dispos.* **27**, 880–886
 17. Floyd, R. A., Kopke, R. D., Choi, C. H., Foster, S. B., Doblas, S., and Towner, R. A. (2008) Nitrones as therapeutics. *Free Radic. Biol. Med.* **45**, 1361–1374
 18. Floyd, R. A., Chandru, H. K., He, T., and Towner, R. (2011) Anti-cancer activity of nitrones and observations on mechanism of action. *Anticancer Agents Med. Chem.* **11**, 373–379
 19. Maples, K. R., Green, A. R., and Floyd, R. A. (2004) Nitrone-related therapeutics: potential of NXY-059 for the treatment of acute ischaemic stroke. *CNS Drugs* **18**, 1071–1084
 20. Krueger, S. K., and Williams, D. E. (2005) Mammalian flavin-containing monooxygenases: structure/function, genetic polymorphisms and role in drug metabolism. *Pharmacol. Ther.* **106**, 357–387
 21. Kato, N., Suzuki, H., Takagi, H., Asami, Y., Kakeya, H., Uramoto, M., Usui, T., Takahashi, S., Sugimoto, Y., and Osada, H. (2009) Identification of cytochrome P450s required for fumitremorgin biosynthesis in *Aspergillus fumigatus*. *Chembiochem.* **10**, 920–928
 22. Steyn, P. S., and Vlegaar, R. (1983) Roquefortine, an intermediate in the biosynthesis of oxaline in cultures of *Penicillium oxalicum*. *J. Chem. Soc. Chem. Commun.* **10**, 560–561
 23. Koizumi, Y., Arai, M., Tomoda, H., and Omura, S. (2004) Oxaline, a fungal alkaloid, arrests the cell cycle in M phase by inhibition of tubulin polymerization. *Biochim. Biophys. Acta* **1693**, 47–55

Novel Key Metabolites Reveal Further Branching of the Roquefortine/Meleagrins Biosynthetic Pathway

Marco I. Ries, Hazrat Ali, Peter P. Lankhorst, Thomas Hankemeier, Roel A. L. Bovenberg, Arnold J. M. Driessen and Rob J. Vreeken

J. Biol. Chem. 2013, 288:37289-37295.

doi: 10.1074/jbc.M113.512665 originally published online November 13, 2013

Access the most updated version of this article at doi: [10.1074/jbc.M113.512665](https://doi.org/10.1074/jbc.M113.512665)

Alerts:

- [When this article is cited](#)
- [When a correction for this article is posted](#)

[Click here](#) to choose from all of JBC's e-mail alerts

This article cites 23 references, 4 of which can be accessed free at <http://www.jbc.org/content/288/52/37289.full.html#ref-list-1>